Characteristics of an annually recurring open-ocean polynya in the Southern Ocean

Soumyadeep Dutta[1,2], P. Sabu[1], Aditya Narayanan[3], Rahul Mohan[1]

[1]National Centre for Polar and Ocean Research, Ministry of Earth Sciences, Headland Sada, Vasco Da Gama, Goa, India.

[2]School of Earth, Ocean and Atmospheric Sciences (SEOAS), Goa University, Taleigao Plateau, Goa, India.

[3]Ocean and Earth Science, University of Southampton, National Oceanography Centre, Southampton, UK.

Corresponding author: Soumyadeep Dutta (Email: soumyadeep@ncpor.res.in)

Key Points:

- Cosmonauts Sea polynya showed strong interannual variability (2002–2023), reaching a maximum extent of ~139,000 km² in August 2016.
- The unusual occurrence of the Cosmonauts Sea polynya caused deep mixing (>400 m), loss of stratification and potential dense water formation.
- The event was driven by anomalous cyclonic wind, positive SAM, and upwelling by vortex stretching due to southward shift of the ACC.

Abstract

Polynyas are within the sea ice cover, typically formed by wind-driven sea ice divergence or upwelling of warm subsurface waters. They play a crucial role in ocean-atmosphere interactions, climate regulation and marine ecosystems by substantially enhancing primary production. Open-ocean polynyas in the Southern Ocean are rare and are typically associated with deep convection, which disrupts conventional circulation pathways and impacts regional heat and carbon budgets. The Cosmonauts Sea (30ºE to 60ºE) is an exception, with open-ocean polynyas forming annually. Using satellite-derived sea ice observations, we examined the spatiotemporal variability of polynyas in this region over the past two decades. The Cosmonauts Sea polynya exhibited large spatial and interannual variability, with the largest event occurring in 2016 (139,000 km²). An Argo float near the polynya recorded deep mixed layers (>400 m) and near-complete erosion of stratification, and the presence of dense water. This event coincided with anomalously intense cyclonic wind stress curl due to synoptic scale storms and a prolonged positive SAM phase (2014-2016), both generally associated with reduced sea ice concentrations. While the southward shift of the Antarctic Circumpolar Current during 2015 acted as a preconditioning mechanism, bringing warmer water towards the polynya region and inducing upwelling by vortex stretching. Additionally, anomalously high shortwave radiative fluxes (~ +20 Wm^{-2}) were observed in the summer preceding the 2016 event. The deep convective mixing observed during this event, together with the presence of dense water, indicates that the Cosmonauts Sea could be a potential dense water formation site.

Plain Language Summary

Polynyas are areas of open water within the sea ice and are categorized into two distinct types: Open-ocean (forming offshore) and Coastal Polynyas (close to the coast). Open-ocean Polynyas in the Southern Ocean are rare; however, a recurring Open-ocean Polynya has been observed in the Cosmonauts Sea, located in the Indian Sector of the Southern Ocean. This feature has been detected regularly since the availability of reliable satellite sea ice data. This repeated occurrence raises questions about its role in absorbing carbon and water mass transformation.

Despite the recurrence of the Cosmonauts Sea Polynya, research dedicated to its study remains limited. In this study, we used an automated image-based feature detection method to detect and track its spatial extent over the past two decades. Our results reveal that the polynya expanded substantially in 2016, making it one of the largest events in recent decades. This unusual occurrence was associated with a prolonged positive phase of the Southern Annular Mode, anomalous cyclonic winds, a southward shift of the Antarctic Circumpolar Current, and strong storms. These findings show that ocean-atmosphere interactions play an important role in creating the extreme sea ice events and sustain this unique polynya.

1 Introduction

Polynyas are regions of open seawater or reduced sea ice surrounded by higher concentrations of sea ice under freezing atmospheric conditions (Barber et al., 2001; Morales Maqueda et al., 2004; Smith et al., 1990). In the Southern Ocean (SO), recurrent polynyas form in specific coastal regions during austral autumn and winter with strong interannual variations in the size and duration (Geddes & Moore, 2007; Smith et al., 1990). Depending on the formation and maintenance mechanisms, polynyas in the SO can be distinguished into two types: Open-ocean polynya and coastal polynya. Coastal polynyas (also called latent heat polynyas) occur in

coastal areas around Antarctica due to the divergence of the sea ice, primarily driven by katabatic winds or ocean currents (Bailey et al., 2004; Tamura et al., 2008). On the other hand, open-ocean polynyas, referred to as 'sensible heat polynyas', develop within the pack ice when cyclonic atmospheric and oceanic circulation causes ice to diverge, leading to the upwelling of warmer water from deeper layers (Goosse & Fichefet, 2001). Even though they occur less frequently than their coastal counterparts, open-ocean polynyas are important regions for climate variability due to their impact on bottom water mass formation (Zanowski et al., 2015), atmospheric circulation (Weijer et al., 2017) and biogeochemistry (Shadwick et al., 2017) of the SO. Hence, understanding the characteristics, formation mechanisms and inter-annual variability of open-ocean polynyas is important to understand the role of SO in the global climate.

The ability to study polynyas was revolutionized in the 1970s with the launch of the Nimbus-5 satellite, which could detect the presence of two significant open-ocean polynyas in the SO. The larger one formed intermittently over the Maud Rise seamount in the Weddell Sea (Cheon & Gordon, 2019), while the smaller one appeared regularly in the Cosmonauts Sea (Wei et al., 2021). Many previous studies (Carsey, 1980; De Lavergne et al., 2014; Gordon & Huber, 1995) have reported the occurrence of the Maud Rise Polynya (MRP) during 1974-1976 due to the ocean eddies generated by the interaction between the ocean currents and the seamount (Holland, 2001). Recent studies (Jena et al., 2019; Narayanan et al., 2024) reported the occurrence of MRP which opened again in 2016 and 2017, highlighting the interaction of atmospheric and oceanic processes such as wind forcing, frictionally driven cross-frontal buoyancy transport, and eddy activity driven by flow-seamount interactions.

On seasonal to decadal timescales, the SO's predominant mode of climatic variability is the Southern Annular Mode (SAM) (Fogt & Marshall, 2020). The SAM or Antarctic Oscillation is the dominant mode of atmospheric variability in the Southern Hemisphere, marked by near-zonally symmetric pressure patterns around Antarctica on intraseasonal to interannual time scales (Fogt & Marshall, 2020). During the positive SAM phase, stronger and poleward shifted westerly winds enhance Ekman divergence at the surface and cause the upwelling of deeper waters (Ferreira et al., 2015). Several previous studies (Cheon et al., 2018; Park et al., 2018) have reported a significant relationship between SAM and polynyas. Polynya formation can be both positively and negatively influenced by the phase of the SAM. A negative SAM phase, characterized by weaker, equatorward-shifted westerly winds, typically brings colder and drier atmospheric conditions over the high-latitudes of SO. This reduces freshwater input, increases surface salinity, and promotes conditions favourable for polynya opening (Gordon et al., 2007). On the other hand, a positive SAM phase strengthens and shifts the westerlies poleward, enhancing precipitation and freshening the surface ocean (-0.05 ± 0.02 PSU near shelf in Indian Sector of Southern Ocean), which can inhibit or limit polynya development (Haumann et al., 2020). In contrast to coastal polynyas, open-ocean polynyas are considered to be rare in the SO (Chu & Gascard, 1991). However, the Cosmonauts Sea Polynya (CSP) recurs almost every year during fall and winter, with potential implications for carbon uptake (Hoppema & Anderson, 2007) and water mass properties (Ohshima et al., 2016). The recurring polynya regions generate new sea ice during this period and hence affect the turbulent heat flux exchange (Tamura et al., 2011), thus influencing the surface energy balance of the SO. Also, such regions are the zones for deep ocean convection, which is a pathway for SO surface waters to densify and sink to the abyss (Cheon & Gordon, 2019). Despite its frequent occurrence, studies on the CSP remain sparse, limiting our understanding of regional variability and dynamics.

The Cosmonauts Sea, situated in the region between 30°E and 60°E, at the eastern end of the Weddell Gyre adjacent to Enderby Land close to Cape Ann, is one of the least studied regions of the SO (Hunt et al., 2007). The circulation system in the Cosmonauts Sea includes three main current systems. The eastward Antarctic Circumpolar Current (ACC) is steered southward by the Southwest Indian Ridge. The westward Antarctic Slope Current (ASC) flows along the continental slope, and the eastern branch of the Weddell Gyre (WGeb), which forms a cyclonic circulation in this region. The ACC is the dominant eastward flow of the SO, transporting large volumes of water and heat. In this region, its southward deflection enhances the delivery of warm Circumpolar Deep Water toward the shelf. The ASC is a narrow, persistent boundary current carrying cold, fresh shelf waters westward, influencing cross-slope exchanges and the export of dense water from the shelf. The CSP is one of the most persistent features in the SO, and it was first reported by Comiso and Gordon in 1987 (Comiso & Gordon, 1987), who subsequently noted that the CSP reoccurred multiple times between 1973 and 1993 (Comiso & Gordon, 1996). They further noted the emergence of two distinct polynya formation modes in this region: the first, known as Eastern Cosmonauts Sea Polynya (eCSP), is limited to the west of 45°E and opens in the early winter, and the second is referred to as Western Cosmonauts Sea Polynya (wCSP) between 50° and 60°E which open in winter or early spring (Morales Maqueda et al., 2004). A recent study showed that the size of the CSP is ~29% smaller than the MRP, but it typically lives nearly twice as long as the MRP (Lin et al., 2024). The study further mentioned that the longer opening of the CSP and its frequent formation in the Cosmonauts Sea shows the significance of this region for the bottom water formation.

The Cosmonauts Sea region features shallow bathymetry and several deep canyons (Harris & Whiteway, 2011), with depths ranging from approximately 2000 to 5000 meters. The ocean currents impinge on this shallow topographic feature and create eddies. These eddies enhance vertical mixing and upwelling of warm, salty water from below the pycnocline (Barthel et al., 2022). The cyclonic wind stress curl associated with the Antarctic divergence drives upwelling, further warming the surface waters and preconditioning the area for polynya formation. Further, the region experiences a close convergence of the eastward flowing ACC and the westward flowing ASC, creating a region of enhanced relative vorticity that requires vortex stretching to conserve potential vorticity. Such vortex stretching is associated with upwelling and has been proposed as a mechanism for the formation of eCSP (Comiso & Gordon, 1996). Upward heat flux over multiple years serves as preconditioning, while divergent winds and storms drive both the advection of ice away from the region and upwelling, acting as immediate triggers for the formation of wCSP (Prasad et al., 2005). The wCSP formed in the Cosmonauts Sea due to the development of embayments in sea ice (a region of open water surrounded by ice on three sides), primarily during the early winter months of June to July. A recent (Wei et al., 2022) found that the presence of a cyclone on the northern boundary of wCSP results in weaker easterly winds in that region and stronger easterly winds at the southern boundary. This leads to weaker southward Ekman flow in the northern boundary and stronger southward Ekman flow in the southern boundary of the wCSP. This increases the meridional heat flow towards the polynya region. Additionally, the difference in flow in the northern and southern boundaries of the polynya promotes the upwelling of warm CDW in the region added by a negative wind stress curl. These two processes aid in the opening of precursor embayments in sea ice, aiding in the

development of wCSP. Between 1979 and 2004, the wCSP and embayments were observed to have a three-year periodicity (Geddes & Moore, 2007).

Despite the recognized importance of open-ocean polynyas, long-term variability in the Cosmonauts Sea Polynya (CSP) remains poorly understood (Geddes & Moore, 2007), and traditional identification methods (Arrigo & van Dijken, 2015; Li et al., 2016; Nihashi & Ohshima, 2015) often fail to capture the open-ocean polynyas due to their short duration and infrequent occurrence (Lin et al., 2024). Furthermore, while the 2016 Maud Rise polynya has been extensively studied (Francis et al., 2019; Narayanan et al., 2024; Zhou et al., 2023), the unusual, largest opening of CSP during the same austral winter has not been examined. This study therefore aims to: quantify the spatial and temporal variability of the CSP over the past two decades (2002-2023) by employing a image segmentation technique on satellite-derived sea ice concentration and understand the oceanic and atmospheric mechanisms responsible for the extreme 2016 opening.

We propose that the multiyear preconditioning due to positive shortwave flux anomaly and southward shift of ACC that transport warmer waters in CSP (Orsi et al., 1995a), also enhance upwelling through vortex stretching(Comiso & Gordon, 1996). This background state, further reinforced by a prolonged positive SAM phase which intensifies cyclonic wind anomaly (Uotila et al., 2013), together with synoptic-scale storm activity (Campbell et al., 2019; Jena et al., 2022), acted as the primary drivers of the extreme polynya opening in 2016, with subsequent impacts on water column structure, deep convection, and potential bottom water formation as revealed by the Argo profiles.

The paper is structured as follows: Section 2 describes the data and image segmentation methodology. Section 3 presents the long-term CSP variability, details of the 2016 event, and analyses the associated hydrographic and atmospheric changes. Section 4 discusses and summarizes the mechanisms driving the 2016 opening, its significance within the long-term context.

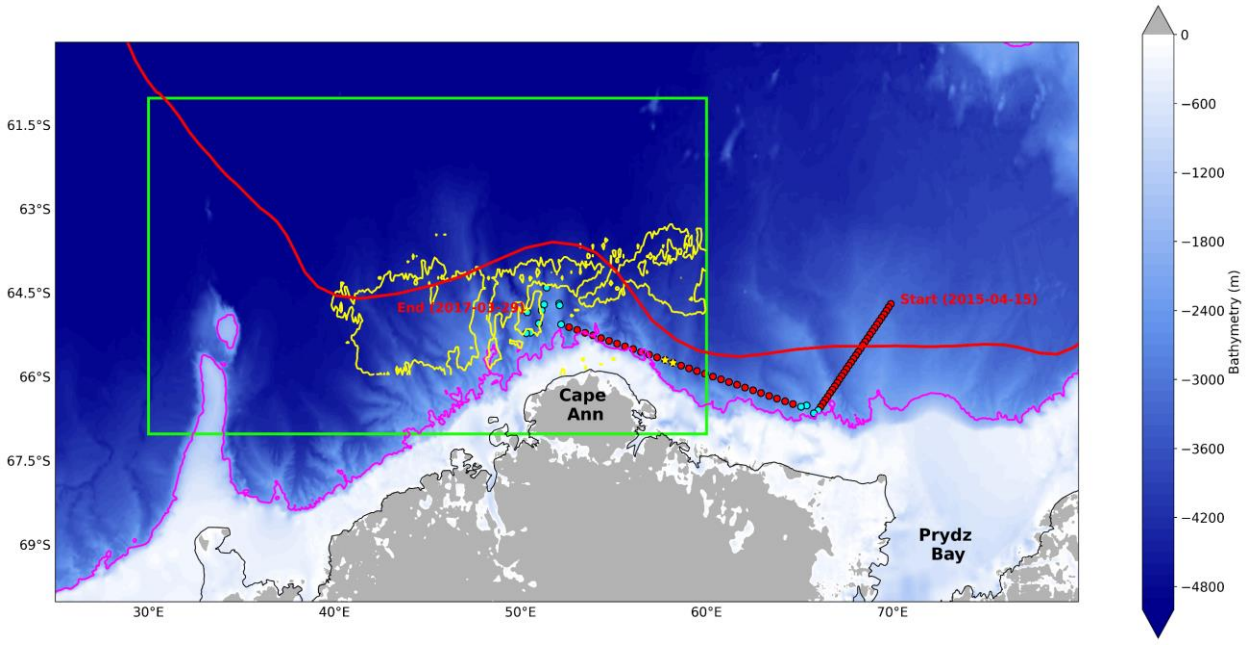

Figure 1. Study Area with General Bathymetric Chart of the Oceans (GEBCO) gridded bathymetry data. The green box shows the location of the Cosmonauts Sea overlayed with 30% SIC contour (yellow) showing the polynya extent during 2016. The Pink contour line show the 2000 m isobath, indicating the general location of the Antarctic Slope Front (ASF) and the red line indicates the Southern Boundary of the Antarctic Circumpolar Current (SB). The red dots indicate the estimated position, and the cyan dots are the true position of the Argo profiles (based on Argo Position data flags, see Hydrographic Data section in Data & Methods) used in the study (Argo id:7900334). The yellow stars indicate the profiles during the 2016 August polynya event.

2 Data and Methods

2.1 Sea Ice Concentration Data

The present study used the daily sea ice concentration (SIC) from the Advanced Microwave Scanning Radiometer (AMSR). To understand the interannual variability of the CSP, we used University of Bremen's AMSR-E (2002-2011) and AMSR-2 (2012-2023) daily data products derived using ARTIST Sea Ice (ASI) algorithm v5.4 on a 6.25 km NSIDC Polar Stereographic grid. The AMSR-E data starts from 1st June 2002 to 4th October 2011, and the AMSR-2 data records start from 2nd July 2012. For the SO, the ASI algorithm performs well with a mean bias of +1.7% against Bootstrap Algorithm (Comiso, 1986) and −1.6% against NASA-Team 2 Algorithm (Markus, 2000) ice concentrations. It shows a high correlation (0.92–0.97), and errors decreasing from ~25% at 0% ice concentration to less than 6% at full ice cover (Spreen et al., 2008a). Prior to this period (2002-2023), robust quantitative analysis of the polynya areas was not possible due to the coarser spatial resolution of satellite sea ice data (~25 km grid) (Campbell et al., 2019).

2.2 Polynya Identification

A modified image segmentation technique was employed to identify the polynya region. In the present study, connected pixels with an SIC of less than 30% that are isolated from the open-ocean are categorized as polynya. Such strict threshold is chosen to avoid the overestimation of the polynya area as ASI SIC data has ~25% error near the marginal sea ice zones. The use of different criteria doesn't impact the study outcome as 2016 is still the largest opening of polynya (Figure S1). The embayments, although considered precursors to polynyas, were not included in the current identification of polynyas since they remain connected to the ocean.

The study employed the scikit-image library (Van Der Walt et al., 2014) to detect polynyas. First, a threshold mask was applied to satellite-derived SIC data to isolate regions with SIC below 30% in the study area. Spatially connected regions of pixels meeting this criterion were identified and labelled. The centroids of these regions were computed, and their geographic coordinates were mapped using the National Snow and Ice Data Centre (NSIDC) Polar Stereographic Grid Information file. Only features whose centroids fell within predefined geographic boundaries (specific to the Cosmonauts Sea study area) were classified as polynya regions. The total polynya extent for a given day was calculated by summing the areas of all qualifying features. Monthly cumulative polynya extent was derived by aggregating daily extents over the month (Text S1).

2.3 Hydrographic Data:

To understand the water column changes before and after the opening of the CSP during 2016, we have used the Argo float [Id-7900334] profiled in the region between (20°E - 70°E) for a period of April 2015-April 2017. To investigate the multiyear preconditioning, mean from Argo profiles were calculated from observations during June–September of 2014–2016 within the region 20°E–70°E and 65°S–70°S. In Argo data, the estimated positions (QC flag = 8) are interpolated locations, whereas the true positions (QC flag = 1 and 2) are the corrected, quality-controlled locations. From the Argo data, Mixed Layer Depth (MLD) is calculated as the depth where the potential density exceeds its surface value by 0.03 kg m^{-3} (Dong et al., 2008). The salinity values are on PSS (Practical Salinity Scale) (Lewis, 1980).

2.4 Radar Altimetry Data:

The along-track sea surface height (SSH) data is sourced from the Centre of Polar Observation and Modelling in collaboration with University College London. This dataset encompasses two satellite altimetry missions: EnviSat, which operated from May 2002 to March 2012, and CryoSat-2, which functioned from April 2010 to October 2018. In regions covered by sea ice, SSH measurements are derived from leads—long, narrow cracks or openings in the ice. Because radar signals can penetrate through open water or thin ice but are largely reflected by thick ice, leads provide crucial "windows" through which altimeters can directly observe the sea surface. To remove the bias, the SSH measurements are levelled according to open-ocean data, following methodologies described by (Dotto et al., 2018).
The offset-corrected data are referenced to the GOCO05c geoid to derive the Dynamic Ocean Topography (DOT). This DOT dataset is gridded onto a regular grid with a resolution of 1° (longitude) by 0.5° (latitude) and smoothed using a Gaussian filter with a 300 km radius. A comprehensive description of the DOT dataset used in this study, along with its validation, is available in Dragomir, 2024.

2.5 Potential Vorticity Conservation:

The persistent formation of the CSP is attributed to a vorticity-induced vertical stretching of the water column, which enhances upwelling of warm deep water and inhibits sea ice formation.

The conservation of potential vorticity is expressed as:

$$\frac{f + \zeta}{h} = Constant$$

Where:

- f is the Coriolis parameter ($f = 2\omega\sin\delta$, with ω being Earth's angular velocity and δ the latitude),
- ζ is the relative vorticity, defined as $\zeta = \frac{\partial v}{\partial x} - \frac{\partial u}{\partial y}$,
- h is the thickness of the water column

The potential vorticity equation is applied at two locations: one at 52.5°E, 64°S, where the ACC and ASC converge near Cape Ann, and another at 40°E, 64°S, outside the convergence zone, in order to assess variations in layer thickness (h) and estimate the upwelling rate associated with vortex stretching.

2.6 Atmospheric Data:

The atmospheric data is averaged over the Cosmonauts Sea region (30° E to 60° E and 60° S to 67° S) (green box in Figure 1). The hourly zonal and meridional components of wind at 10 m and Mean Sea Level Pressure (MSLP) with a 0.25° resolution are obtained from ECMWF ERA-5 reanalysis for the period (2002-2023). The sea ice stress on the atmosphere is not considered in the study. The wind stress is calculated as:

$$\tau_x = 1.225\rho\, C_D u\, |u|$$

$$\tau_y = 1.225\rho\, C_D v\, |v|$$

Where, ρ is the density of air (1.225 kg m^{-3}), C_D is the Wind Drag Coefficient (1.3×10^{-3}), u & v are the zonal and meridional velocity of winds.

Wind stress curl is computed as:

$$\nabla \times \tau = \frac{\Delta\tau_y}{\Delta x} - \frac{\Delta\tau_x}{\Delta y}$$

Mean Radiative (shortwave and longwave) and turbulent (sensible and latent) heat flux data spanning 2002–2023 were obtained from the ECMWF ERA-5 reanalysis product at a spatial resolution of 0.25° × 0.25°, averaged over the Cosmonauts Sea region (30° E to 60° E and 60° S to 67° S), resampled to daily intervals for heat flux analysis. The Net Heat Flux was computed as the sum of radiative and turbulent fluxes. The heat flux anomalies were derived by subtracting the corresponding monthly climatological mean values.

The total column water vapour, which can be used as Integrated Water Vapour (IWV)(Mo, 2024), was obtained from ERA-5 reanalysis for the same period (2002-2023) at the same spatial resolution as other atmospheric data to check the influence of IWV on the CSP formation.

In this study, storm events are defined as one or more grid cells in the Cosmonauts Sea region with wind speeds greater than 20 m/s or MSLP below 960 hPa based on hourly ERA5 wind and MSLP data (Campbell et al., 2019).

3 Results

3.1 Interannual variability of the CSP

An analysis of relatively high-resolution, remotely observed sea ice concentrations (6.25 km grid; see Methods) during the past two decades (2002–2023) revealed that polynya formation in the Cosmonauts Sea was a recurring phenomenon during austral winters (Figure 2a), predominantly involving the opening of the wCSP. The development of wCSP was observed more frequently during this period, except in the years 2002, 2008, 2012, 2016, 2017, and 2022, when the eCSP formed instead. Additionally, the eCSP formed in the years 2003, 2011, 2019, and 2023, often preceded by wCSP events. Notably, the wCSP occurred annually after 2016, except in 2020, whereas the eCSP appeared intermittently, sometimes preceding or coinciding with wCSP events. Large interannual variability in the formation months of the wCSP and eCSP and its area was also noticed during the study period

In 2006, the wCSP first opened in mid-June (Figure 2b) with an area of ~70×10^3 km^2 and closed by early July. Whereas in 2008, it opened in mid-July (Figure 2c) and stayed open (area ~84×10^3 km^2) until early October. In 2011, the eCSP opened in September, preceded by a wCSP event in July (Figure 2d). In 2013, eCSP stayed open from late June (Figure 2e) to early July, reaching a maximum extent of ~98×10^3 km^2 at the end of July, with simultaneous opening of both wCSP and eCSP on the 27th of June (Figure 2e). In 2019 and 2020 (Figure 2g&h), eCSP opened in July (~84×10^3 km^2) followed by a weak wCSP event in September. In 2023, an embayment within sea ice started forming in the western Cosmonauts Sea in June, leading to a small wCSP in late July. In August, an unusual eCSP developed from an embayment—something not typically observed. By September (Figure 2i), a large polynya covering both the wCSP and eCSP had opened, becoming the largest Cosmonauts Sea polynya since 2016 (Figure 2f).

The analysis showed that the wCSPs typically form in winter (June-July) and are preceded by the formation of an embayment in sea ice. While the eCSPs generally opens in late winter (August-September) directly without initially forming an embayment in sea ice. The analysis during the above period also showed that one of the most extensive openings of the CSP occurred in 2016. In our long-term analysis, we were unable to clearly isolate the distinct oceanic mechanisms driving the eCSP and wCSP. The two regions do, though, exhibit distinct relations with cyclonic winds, which are discussed in a later section. However, studying the oceanic mechanisms remains challenging due to the limited availability of ocean observations in this region. Further, we maintain consistency with previous studies (Geddes & Moore, 2007; Prasad et al., 2005; Wei et al., 2022) in this region that do not differentiate between the western and eastern polynyas, with the majority focusing predominantly on the wCSP. Hence, the subsequent sections of this paper focus on examining the potential drivers behind the anomalous event in 2016, treating the western and eastern polynyas as a single system, unless otherwise specified.

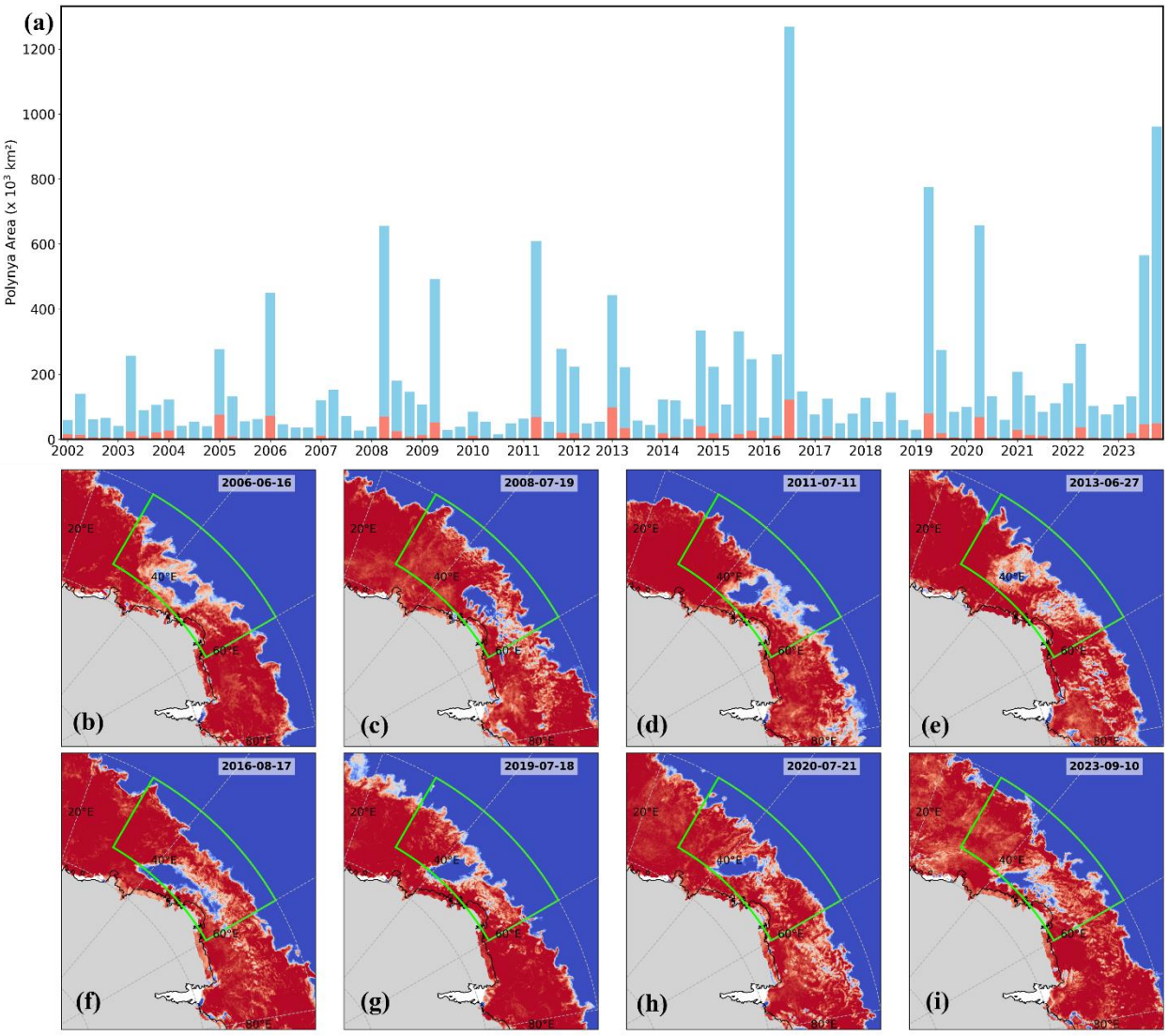

Figure 2. **(a)** shows the cumulative extent of each month (blue bar) and maximum polynya extent for the particular month (orange bar) of the CSP events in winter months. **(b)-(i)** shows some of the large CSP events in the last two decades with Cosmonauts Sea region highlighted by the green box.

3.2 Unusual occurrence of CSP during 2016

The CSP formation in 2016 was highly anomalous (~ 7.5 times higher than the climatological mean polynya area) in its area compared to polynya events observed in the Cosmonauts Sea over the last two decades. It was marked by the largest polynya extent and a simultaneous opening of wCSP and eCSP. Many small polynyas started appearing in the Cosmonauts Sea region in July and these features were closed by sea ice by the end of the month (Figure S2). During 2016, the CSP reached an extent of ~139×10^3 km^2 and a cumulative extent (time-integrated monthly area; see Methods) of ~1270×10^3 km^2, and stayed open till 4th September.

The 2016 polynya event began on 4th August with the first opening in the eastern Cosmonauts Sea (~54°E & 61°S), covering an area of ~12 × 10^3 km^2. On 8th August, it expanded to ~17×10^3 km^2, but closed the following day. On the same day, a polynya began forming in the western Cosmonauts Sea (~40°E), which subsequently spread across the region from 40°E to 60°E. By 11th August it achieved the largest area (~139×10^3 km^2) observed in the Cosmonauts Sea over the study period of 2002 to 2023. Following this, the polynya started shrinking, closing completely on 5th September. The analysis showed that the 2016 CSP event lasted for over a month and had a cumulative (time-integrated) open water area of ~1270 × 10^3 km^2, making it one of the most extraordinary events recorded in the Cosmonauts Sea over the last two decades.

3.3 Oceanic Condition during the 2016 CSP event

To understand how water column properties varied before and after the anomalous opening of the CSP during 2016, we used an Argo float (Id: 7900334) that profiled in the region between 20°E and 70°E. The trajectories of the float are marked in Figure 1. During August 2016, when the CSP was active, the estimated position of the Argo float was very close to the active polynya region. This is further confirmed through the observed deep mixing, with the mixed layer deepening to depths exceeding 400 m (white line in Figures 3a and 3b), which is only possible near the polynya.

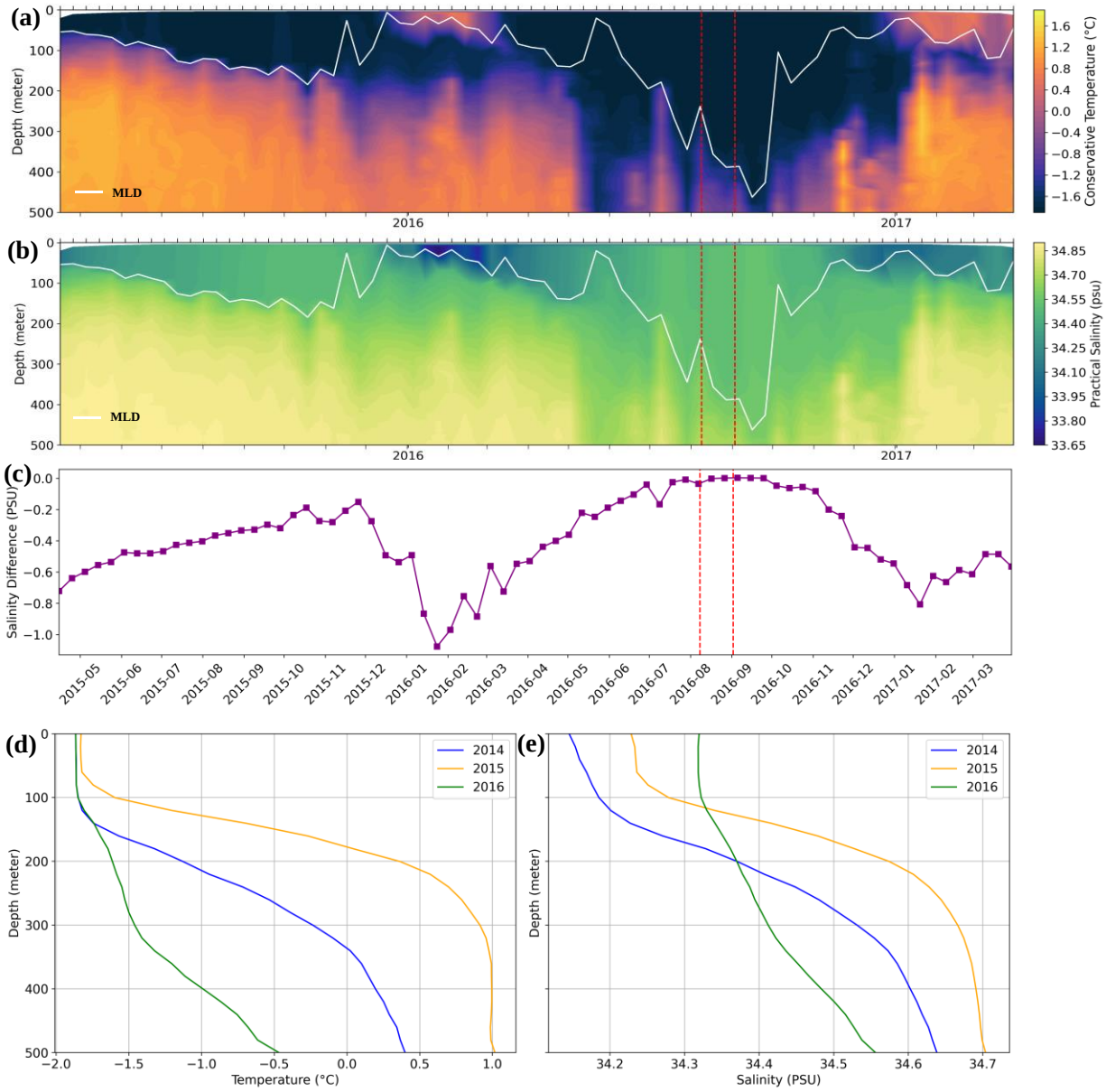

Figure 3. Oceanic condition during 2015-16 in Cosmonauts Sea. **(a)** temperature, **(b)** salinity, **(c)** the salinity difference between mixed layer salinity and salinity at 250 meters depth. The white line indicates the MLD and the red vertical lines indicate the start and end of the polynya event. **(d)** Mean Temperature and **(e)** Mean Salinity vertical profile for 2014 (Blue), 2015 (Green) and 2016 (Orange), computed from all available Argo profiles during JJAS of each respective year.

Prior to the opening of the polynya in February 2016, the MLD (white line in Figure 3a and 3b) was shallow (~50m) with a mixed layer temperature of ~0.5°C and the presence of comparatively fresh surface waters in the mixed layer with a salinity less than 34 (Figure S3a). As the season advanced, surface waters cooled and salinity increased (>34.4) and was most likely driven by atmospheric cooling and brine release from sea ice formation. This salinification may have been further amplified by the upward mixing of saltier Circumpolar Deep Water

(CDW) (S > 34.5, $\theta \geq 0$) from beneath the pycnocline (Figure S3b). In the subpolar SO, stratification is primarily controlled by salinity (Roquet et al., 2022). We use the difference between the mixed layer salinity and salinity at 250 m depth (typically located below the pycnocline) as a proxy for stratification. We found that this difference had gone from (~-1) at the start of 2016 to nearly vanishing (~0) during the active phase of the CSP compared to the previous winter (~-0.3, Figure 3c). This increase in mixed-layer salinity reduced the stability of the water column, aiding the vertical mixing of heat and salt. The heat most likely mixed in from below the MLD is then lost to sea ice and the atmosphere, cooling and freshening the subsurface CDW. The deepening of the MLD and the resulting weakening of the stratification after the anomalous opening of the CSP indicated strong convection in the region. The stratification below the mixed layer strengthened once again by February 2017. The mixed layer properties in the vicinity of CSP differed substantially, particularly between 2015 (-1.79°C, 34.23; averaged from June to September) and 2016 (-1.85°C, 34.32; averaged from June to September), indicating a colder and saltier mixed layer that brought about a weakly stratified water column which led to the formation of polynya in 2016 (Figure 3a). The subsurface computed from all available Argo profiles during JJAS (2014-2016) of each respective year shows that the temperature (0.87°C) and salinity (34.66) during 2015, higher than 2014 values (0.87°C, 34.54) (Figure 3d, e), show a heat storage in the subsurface which may have aided the polynya opening in 2016. The MLD during the active phase (June-October) of 2016 CSP exceeded 400 m (Figure 3a, b), nearly twice that of the previous winter. Dense bottom waters, typically found at greater depths before and after the event, revealed their presence at shallower depths during the polynya's peak (Figure S3a, b). This vertical redistribution indicates active dense water formation within the polynya, potentially making this site an important region for deep ocean ventilation (Figure S3c). Future studies incorporating more observations and model simulations are needed to explore this further.

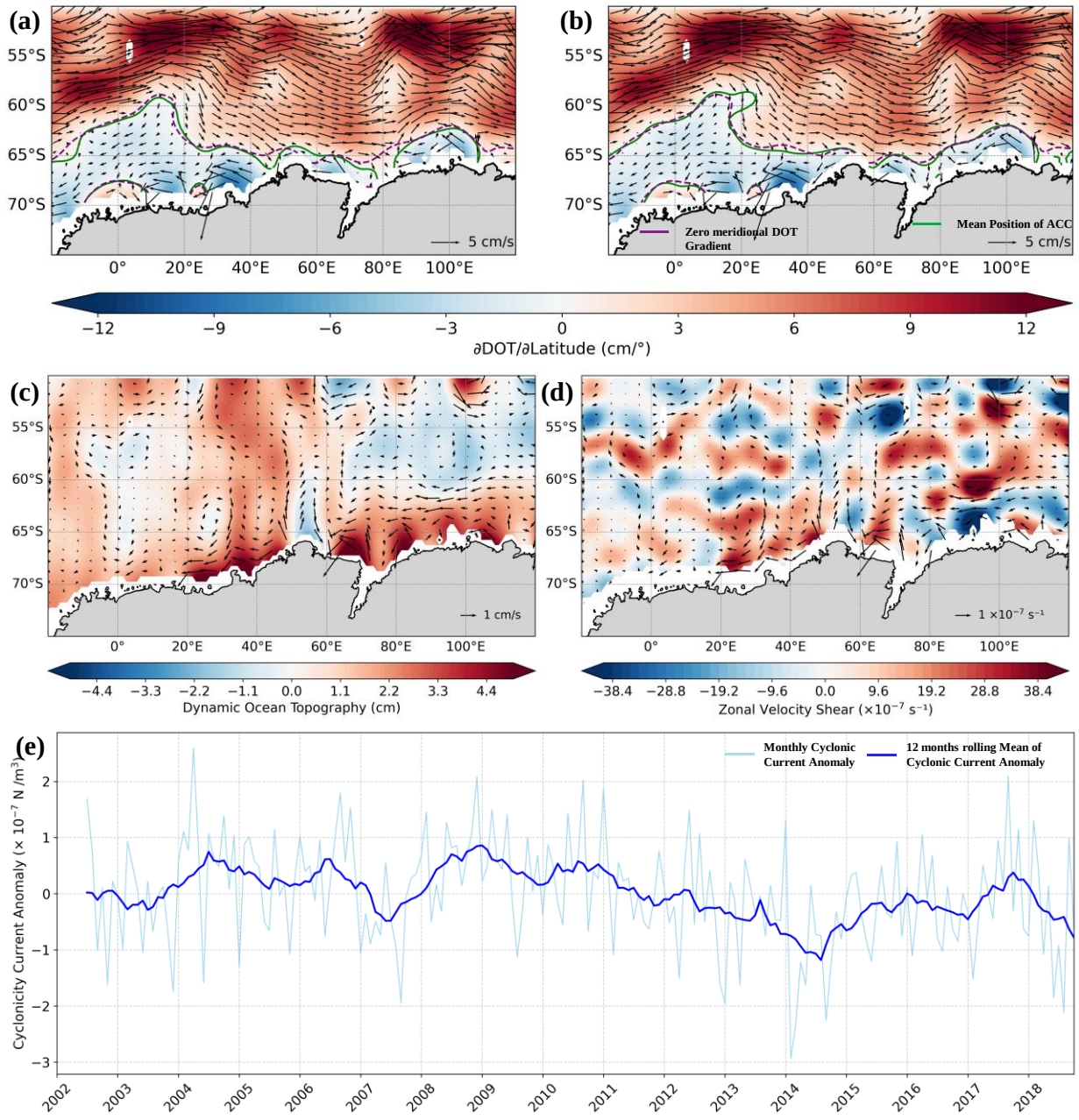

Figure 4. June–September (JJAS) mean surface geostrophic currents (arrows) and meridional gradient of dynamic ocean topography (DOT; colours) for (a) 2015 and (b) 2016. Purple contours mark the zero meridional gradient of DOT, indicating the climatological mean position of the Antarctic Circumpolar Current (ACC), while green contours show the ACC position for each respective year. (c) Difference in DOT (colours) and geostrophic currents (arrows) between composites of years in the upper and lower 20th percentiles of polynya area. (d) Same as (c), but for zonal velocity shear (colours) and geostrophic currents (arrows). (e) Cyclonicity of surface currents averaged over 30°E–60°E, 60°S–80°S.

To gain insight into the ocean currents of the Cosmonauts Sea, we use satellite-driven DOT data and analyzed the surface geostrophic currents. The JJAS climatology of DOT is

calculated for 2002-2018. In 2015, the position of the ACC, as indicated by the zero meridional DOT gradient contour, reveals a southward shift in Cosmonauts Sea region relative to its climatological mean position (Figure 4a). This shift suggests an increase in warm CDW near the CSP region during 2015, as the southward shift of the ACC transports CDW poleward. Further, during July 2016, the ACC shows a strong southward anomaly near Cape Ann (Figure 4c) which brings warmer waters to the region. Similar southward anomaly near CSP region can be observed in August of 2016 (Figure 4d) which may also bring warm waters aiding the polynya. By comparing the difference plots between the top 20th and bottom 20th percentile polynya area years, it is evident that during large polynya years, the surface currents within the CSP region are predominantly southward (Figure 4e–f). This southward transport indicates that ocean currents play a critical role in advecting warmer waters into the polynya region, thereby enhancing conditions favorable for polynya formation. Furthermore, the presence of a positive zonal velocity shear in the Cosmonaut polynya region (Figure 4f) suggests a strong horizontal convergence between the ACC and the ASC. This convergence intensifies the horizontal shear, which, through the principle of vortex stretching, drives upwelling. The horizontal convergence must be balanced by vertical extension of the water column. This process amplifies the relative vorticity, leading to a compensating upward motion of deeper waters. Such dynamics are particularly important in regions of strong current interaction, where they facilitate the vertical transport of CDW toward the surface. The estimated upwelling rate (Comiso & Gordon, 1996) during JJAS 2015, when the ACC exhibited a marked southward shift, reached 8.34×10^{-6} cm s^{-1}, one of the highest values observed across the study period. More broadly, upwelling rates in the region consistently range between $7–9 \times 10^{-6}$ cm s^{-1}, underscoring the significance of vortex stretching as a persistent mechanism for supplying oceanic heat to the surface and sustaining polynya activity in the Cosmonauts Sea.

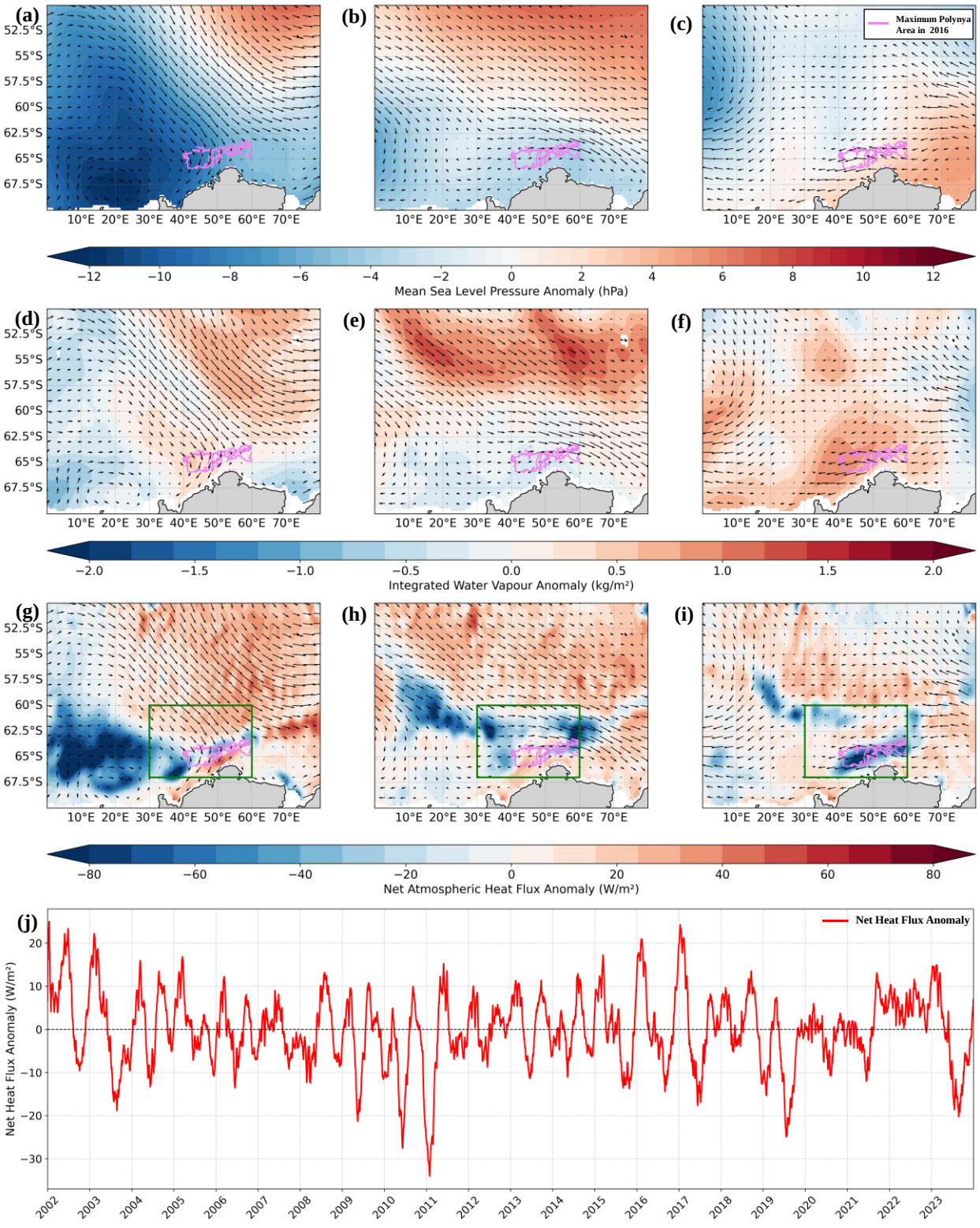

Figure 5. Atmospheric state averaged during June (column 1), July (column 2), and August (column 3) of 2016: **(a-c)** Mean sea level pressure **(**MSLP), **(d-f)** integrated water vapour (IWV), and **(g-i)** net atmospheric heat flux. All mapped fields are shown as anomalies against their

monthly climatology, with overlaid wind vectors. The violet contour shows the maximum polynya area during August 2016. **(j)** Spatially averaged net atmospheric heat flux in the green box (CSP region) shown in (g-i) computed using a rolling mean with a window of 90 days.

3.4 Atmospheric conditions

To investigate the role played by the atmosphere in the formation of the 2016 polynya, we now turn our attention to the MSLP, IWV, and the net surface heat flux. In early 2016, there was a large positive anomaly in the Net Heat Flux measuring 20 W m^{-2} (Figure 5j), which was facilitated by an anomalous shortwave heat flux of 30 W m^{-2} (Figure S4c), that acted to warm the surface ocean. Similar kind of condition can be observed during early 2015 with 25 W m^{-2} shortwave heat anomaly (Figure S4c). This heat was absorbed and stored within the ocean. This can warm the subsurface ocean and inhibit sea ice growth. Subsequently, during the appearance of the 2016 polynya, the latent heat (-6 W m^{-2}), sensible heat (-6 W m^{-2}), and longwave heat (-2.5 W m^{-2}) fluxes exhibited negative anomalies (Figures S4a, b, c), consistent with greater heat loss to the atmosphere due to the loss of the insulating sea ice cover. During this period, the net heat flux dropped to -15 W m^{-2}, indicating a net transfer of heat from the ocean to the atmosphere. Similar negative fluxes were observed during other major polynya events, including those in 2010, 2019, and 2023—some of the largest events following 2016. This recurring pattern links sustained negative heat fluxes to winter polynya activity in the Cosmonauts Sea, where open water enables efficient heat exchange.

The atmospheric conditions in 2016 functioned as short-term drivers for the unusual opening of CSP. In June, an intense low-pressure system centered at about 20ºE and 68ºS had formed with MSLP anomalies falling below -12 hPa (Figure 5a). The low-pressure system drove an intense poleward flow of warm (Figure 5g), humid (Figure 5d) subtropical air mass over the CSP region. This poleward flow eased in July but reemerged in August when once again warm (Figure 5i) and humid (Figure 5f) air masses were transported over the CSP region. Water vapour in the atmosphere affects heat flux in the region (Figure 5g,h) as enhanced moisture leads to enhanced downward longwave radiation, resulting in a positive net heat flux anomaly over the CSP region during June and August. Further, during the polynya event in August, a notable negative heat flux anomaly of -80 W m^{-2} was recorded directly over the location of the polynya opening (Figure 5i), indicating substantial heat loss from the ocean.

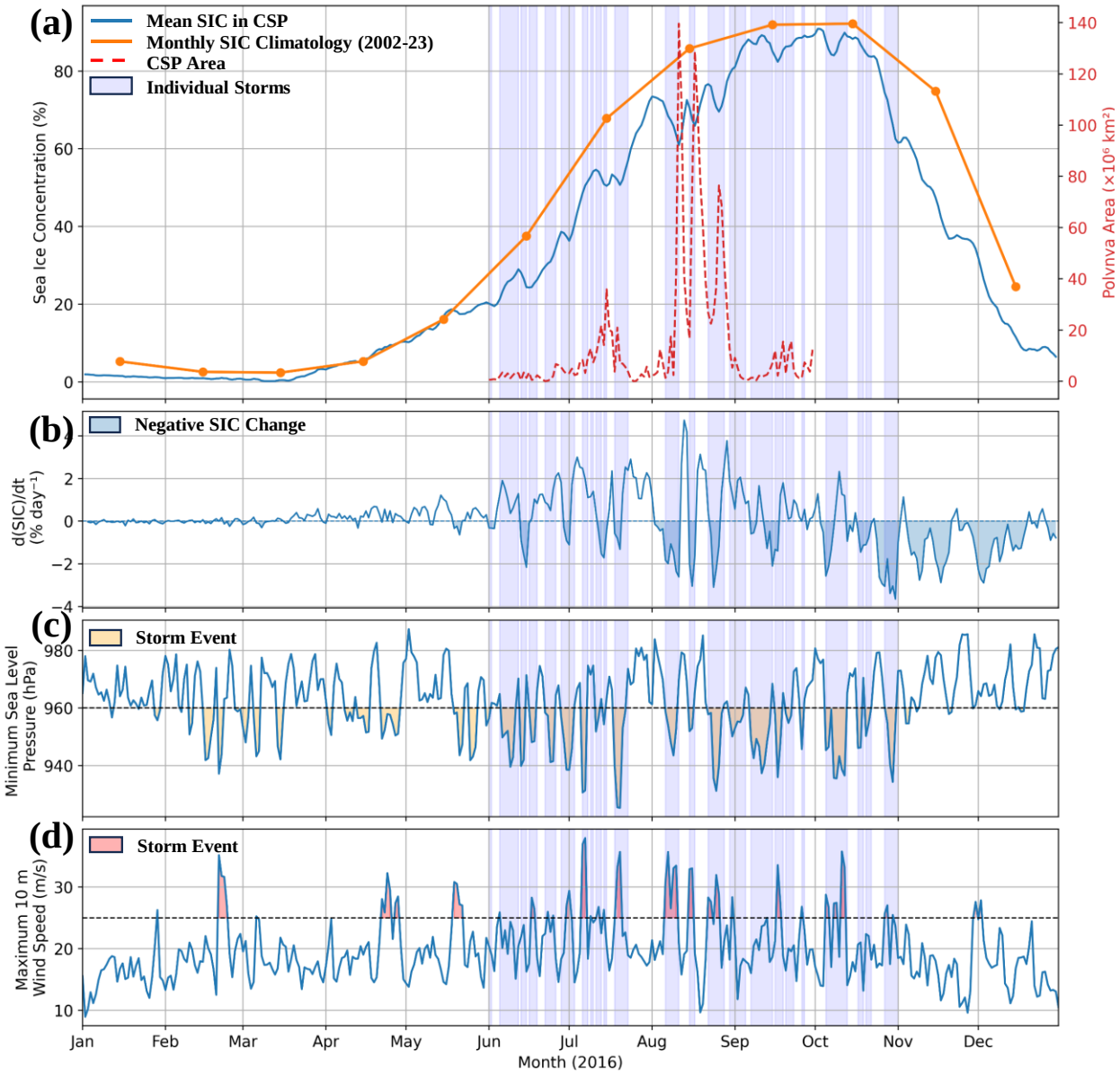

Figure 6. (a) The mean daily SIC in the Cosmonauts Sea region (30°-60°E, 60°-67°S) in blue. Monthly SIC climatology from 2002-2023 is shown with orange line and the calculated polynya area is shown in red. **(b)** The daily change in SIC with negative changes highlighted in blue. **(c)** The daily minimum MSLP with yellow highlighted region identified as storm events and **(d)** The daily maximum wind speed with red highlighted regions identified as storm events (see Data & Methods, Section 2)

Synoptic-scale storms may have played an important role in both the opening and sustenance of the CSP. The major sea ice loss events (Figure 6b) are closely associated with the deepening of MSLP (Figure 6c) and increased wind velocity (Figure 6d). Furthermore, daily wind stress curl analysis during 2016 revealed that peaks in polynya extent coincided with large negative wind stress curl events (Figure S5). A significant correlation ($r = 0.6$, $p < 0.0001$) was

found between the daily wind stress curl and sea ice concentration anomalies during June to September, 2016, which is notably stronger than the correlation over the 2002-2023 period ($r = 0.189$; $p < 0.0001$). Spatial wind variability revealed a strong cyclonic pattern preceding the peaks in polynya extent, particularly on August 11th, 17th, and 27th (Figure S5).

The first peak in polynya area was associated with an SLP of ~940 hPa (Figure 6c) and wind speeds up to 35 m/s (Figure 6d). Similarly, the subsequent two peaks were also driven by deep low-pressure systems and strong winds. Notably, during the final peak, the SLP dropped below 940 hPa, with wind speeds reaching ~30 m/s (Figure 6). These observations highlight the close relationship between storm events and the expansion of the polynya area. During the period 2002–2023, SAM exhibited a strong negative correlation with MSLP ($r = –0.74$, $p < 0.0001$) and a positive correlation with wind stress curl ($r = 0.54$, $p < 0.0001$) (Figure S6), which indicate that SAM may positively impact the polynya opening.

4 Discussion and Conclusion

The analysis of sea ice over the past two decades showed pronounced spatial and temporal variability in the formation of polynyas in the Cosmonauts Sea. Previous studies have also highlighted the interannual variability in the location of the open-water polynyas in this region, as well as the regular occurrence of wCSP events during late autumn and early winter (Comiso & Gordon, 1996; Wei et al., 2021). Many studies have reported the formation of CSP during winter but none have focused on its long-term variability. In the present study, we have used a new image segmentation technique to identify both the wCSP and eCSP, revealing their variability over the last two decades. The CSP opened every year over the last two decades (Figure 2a) with large interannual variation in its area. Our findings indicate that the wCSP events were more frequent before 2016, whereas the eCSP events became more regular afterwards. After 2016, the eCSP opened almost every year except in 2020. We also noticed the unusually large polynya in 2016 with an area that was 7.5 times larger than the long-term average. During the anomalous polynya event of 2016, both wCSP and eCSP opened at the same time which resulted in the largest CSP opening with a cumulative (time-integrated) extent of ~1270×10^3 km^2 and a maximum extent of ~139×10^3 km^2. During this event the mixed layer reached ~480 m, with a mixed layer temperature of ~-1.8°C and a high mixed layer salinity of 34.4 accompanied by a near-zero salinity difference between the surface and the subsurface (Figure 3), suggesting deep mixing. During this event, heat and salt from upwelled CDW warmed and salinified surface waters while cooling and freshening the CDW (Figures S3a, b). Notably, dense bottom waters were observed at shallower depths during the period when the polynya opened up, which may indicate new dense water formation. However, further investigations using more extensive observations and model simulations will be required to address this in the future.

Several atmospheric and oceanographic processes play a role in the unusual occurrence of polynya during 2016. Near Cape Ann, the opposing ACC and ASC converge, resulting in enhanced zonal shear between them (Figure 4). This narrowing amplifies the water column's relative vorticity. To conserve PV ($(f+\zeta)/h$; a ratio of planetary and relative vorticity and the water column height), an increase in relative vorticity results in the vertical stretching of the water column, upwelling warm, salty CDW towards the surface. The upwelling CDW enhances vertical heat transport towards the surface, reducing sea ice and also suppressing the formation of

new sea ice (Comiso & Gordon, 1987; Yang et al., 2024). During the analysis, we noticed that, in 2015, the ACC moved southward relative to its long-term mean position indicated by the southward excursion in the green contour line in Figure 4a., This poleward movement of the ACC enables a greater intrusion of warm CDW towards the CSP region as the ACC is the main source of CDW in the subpolar SO (Orsi et al., 1995b). At the same time, the narrowing of the region between the ACC and the ASC induces upwelling via vortex stretching as explained above, which further helps bring CDW near the surface. We compute the rates of upwelling driven by the vortex stretching mechanism, as explained in Section 2, to consistently range between $7–9 \times 10^{-6}$ cm s^{-1}, underscoring the importance of vortex stretching as a persistent mechanism for supplying oceanic heat to the surface. The strength of the ACC can be linked to the SAM, where a positive SAM is associated with a poleward shift in the westerlies wind belt, which may have helped in the poleward intrusion of warmer water (Sallée et al., 2008). It was also noticed that SAM stayed in a prolonged positive phase from 2014 and reached the strongest positive phase (SAM Index=4; Figure 4c) during the 2016 polynya. In 2014, Weddell Gyre also spins up, manifesting as an anomalous cyclonic flow in the CSP region exhibited (Figure 4e) which may have brought heat and salt closer to the base of the mixed layer. A positive net heat flux anomaly was observed during the summers of 2015 (18 W m^{-2}) and 2016 (20 W m^{-2}) (Figure 5j), mainly driven by anomalous shortwave heat fluxes of 20 W m^{-2} and 22 W m^{-2}, respectively (Figure S4). This excess incoming heat can be absorbed and stored in the ocean (Maykut & McPhee, 1995; Maykut & Perovich, 1987; Perovich & Richter-Menge, 2000), forming a subsurface heat reservoir that inhibits sea ice growth and preconditions the water column for polynya formation. Evidence of this subsurface warming was captured by multiple Argo floats in the region, which recorded a JJAS mean subsurface (200–500 m) temperature and salinity of 0.87 °C and 34.66 in 2015—higher than the 2014 values of –0.16 °C and 34.54. Simultaneously, the surface (0–50 m) salinity increased from 34.15 in 2014 to 34.23 in 2015 and 34.32 in 2016, reducing the stability of the water column. The inhibition of sea ice growth is reflected in the development of the largest summer polynya in November 2015, with a cumulative area of 1650×10^3 km^2, driven by the early retreat of sea ice. Furthermore, the shallow bathymetry near Cape Ann may have amplified upwelling through eddy shedding—a process where mesoscale eddies interact with topographic slopes, generating vertical water displacement (Thompson et al., 2014). Such eddy–topography interactions can enhance the upward transport of warm subsurface waters (Stammer, 1998), potentially sustaining polynya activity.

The atmospheric anomalies during 2016 played a pivotal role in initiating and sustaining the CSP, highlighting the importance of short-term atmospheric forcing. In June, an MSLP anomaly of approximately 8 hPa developed northeast of the Cosmonauts Sea at a characteristic Zonal Wave 3 (ZW3) ridge position, while a strong negative anomaly of less than –12 hPa was observed near the coast at a ZW3 trough node (Figure 5a). By July, the positive anomaly expanded across the northern region and the coastal negative anomaly weakened to around –2 hPa (Figure 5b). This persistent ridge-trough dipole—a signature of the amplified ZW3 pattern—established a steep meridional pressure gradient that generated persistent southward winds channelled between the high and low pressure centers. These winds efficiently advected warm, moist air from lower latitudes, as indicated by the positive IWV anomalies in June and July (Figure 5d, e), which closely mirrored the SLP patterns. These moist conditions enhanced longwave absorption in the atmosphere, reducing outgoing radiation and contributing to a net surface heat gain, evidenced by the positive net heat flux anomalies during these months (Figure

5g, h). However, during the main polynya event in August, a strong negative net heat flux anomaly of –80 W m^{-2} was recorded directly over the polynya region (Figure 5i), indicating substantial ocean heat loss. Notably, earlier in 2016, net heat flux anomalies reached 20 W m^{-2} (Figure 5j), suggesting preconditioning through ocean heat storage partially enabled by prolonged, ZW3-driven atmospheric heat transport. During the polynya's expansion, latent (–6 W m^{-2}), sensible (–6 W m^{-2}), and longwave (–2.5 W m^{-2}) fluxes also showed negative anomalies (Figure S4a–c), consistent with enhanced heat loss due to the absence of insulating sea ice.

In parallel, synoptic-scale storms were closely tied to major sea ice loss events (Figure 6), with each peak in polynya area coinciding with intensified low-pressure systems (MSLP < 960 hPa) and high wind speeds (up to 35 m/s; Figures 6c and 6d). These events were associated with strong negative wind stress curl anomalies (Figure S5), facilitating sea ice melt by drawing warmer subsurface water to the surface. A robust correlation was found between daily wind stress curl and sea ice concentration anomalies during June to September in 2016 ($r = 0.6$, $p < 0.0001$), far stronger than the long-term mean ($r = 0.189$, $p < 0.0001$). Regionally, the eCSP exhibited a much stronger correlation ($r = 0.29$, $p < 0.0001$) than the Western sector ($r = 0.06$, $p = 0.004$), indicating that cyclonic wind forcing plays a more important role in driving eCSP formation and that the 2016 polynya primarily followed this mechanism. Furthermore, over the period 2002–2023, SAM exhibited a strong negative correlation with MSLP ($r = –0.74$, $p < 0.0001$) and a positive correlation with wind stress curl ($r = 0.54$, $p < 0.0001$), based on time series smoothed with a 1-year rolling mean to suppress short-term variability (Figure S6), emphasizing the role of large-scale climate variability in modulating storm activity and associated polynya dynamics. Together, these results demonstrate that the 2016 CSP event was driven by a combination of anomalous atmospheric moisture, radiative forcing, and storm-induced ocean-atmosphere interactions, linking synoptic and climatic scales in shaping polynya behaviour.

The findings of this study reveal that the formation and variability of the Cosmonaut Sea Polynya (CSP) are governed by a complex interplay of atmospheric, oceanic, and climatic processes operating across multiple timescales. The anomalous 2016 event in CSP exemplifies how enhanced vortex stretching, driven by the convergence of the ACC and ASC near Cape Ann, together with a prolonged positive phase of the SAM and an intensified ZW3 pattern, can precondition the upper ocean through increased heat and salt fluxes from upwelled CDW. These processes, compounded by positive summer heat flux anomalies and synoptic-scale storm activity, collectively contributed to deep convective mixing and the largest recorded CSP opening in recent decades. In general, this study highlights the crucial role of both large-scale climate modes and short-term atmospheric variability in modulating polynya formation, persistence, and intensity, providing new insights into the mechanisms driving deep ocean ventilation and upper-ocean heat exchange in the Antarctic zone. Detailed future studies by integrating satellite data, observations, and models are needed to fully explore the various processes responsible for the formation of the CSP and the possible dense water formation in this region.

Acknowledgements

We thank Dr. Thamban Meloth, Director National Centre for Polar and Ocean Research (NCPOR), for his support and encouragement. We acknowledge the funding support from

the Ministry of Earth Sciences (MoES), India. We also acknowledge three anonymous reviewers for their valuable suggestions that helped to improve the manuscript. We acknowledge the international Argo program. This research is a part of the Indian component of the CRiceS (Climate Relevant interactions and feedbacks: the key role of sea ice and Snow in the polar and global climate system) project. This is a NCPOR contribution no. XX-XXXX

Open Research

The codes used in the study are available at (Dutta, 2025). Southern Ocean bathymetry data was obtained from IBCSO v2 with a spatial resolution of 500 meters (Dorschel et al., 2022) from https://doi.pangaea.de/10.1594/PANGAEA.937574. Sea-ice concentration data at 6.25 km resolution for the period 2002-2023 is obtained from the University of Bremen ASI v5.4 AMSR-E and AMSR2 products (Spreen et al., 2008b) at https://seaice.uni-bremen.de/sea-ice-concentration/amsre-amsr2/information/. The NSIDC Polar Stereographic Ancillary Grid Information downloaded at https://nsidc.org/data/nsidc-0771/versions/1/. The station based SAM index data is obtained from https://climatedataguide.ucar.edu/climate-data/marshall-southern-annular-mode-sam-index-station-based. The temperature and salinity profiles of Argo float 7900334 are obtained from Argo GDAC (Wong et al., 2020) at https://www.seanoe.org/data/00311/42182/. The Dynamic Topography Data at 0.5° (latitude) and 1° (longitude) resolution was obtained from https://doi.org/10.5258/SOTON/D3006/. Daily ERA 5 atmospheric reanalysis data for the period of 2002-2023 is downloaded using CDS Python API from https://doi.org/10.24381/cds.adbb2d47.

Conflict of Interest Statement

The authors declare no conflict of interest.

References

Arrigo, K. R., & van Dijken, G. L. (2015). Continued increases in Arctic Ocean primary production. *Progress in Oceanography*, *136*, 60–70. https://doi.org/10.1016/J.POCEAN.2015.05.002

Bailey, D. A., Lynch, A. H., & Arbetter, T. E. (2004). Relationship between synoptic forcing and polynya formation in the Cosmonaut Sea: 2. Regional climate model simulations. *Journal of Geophysical Research: Oceans*, *109*(C4), 4023. https://doi.org/10.1029/2003JC001838

Barber, D., Marsden, R., Minnett, P., Ingram, G., & Fortier, L. (2001). Physical processes within the North Water (NOW) polynya. *Atmosphere - Ocean*, *39*(3), 163–166. https://doi.org/10.1080/07055900.2001.9649673/ASSET//CMS/ASSET/45CA29AA-2F04-4E7E-B55B-6DEA61F91832/07055900.2001.9649673.FP.PNG

Barthel, A., Hogg, A. M., Waterman, S., & Keating, S. (2022). Baroclinic Control of Southern Ocean Eddy Upwelling Near Topography. *Geophysical Research Letters*, *49*(7), e2021GL097491. https://doi.org/10.1029/2021GL097491

Campbell, E. C., Wilson, E. A., Moore, G. W. K., Riser, S. C., Brayton, C. E., Mazloff, M. R., & Talley, L. D. (2019). Antarctic offshore polynyas linked to Southern Hemisphere climate anomalies. *Nature 2019 570:7761*, *570*(7761), 319–325. https://doi.org/10.1038/s41586-019-1294-0

Carsey, F. D. (1980). Microwave Observation of the Weddell Polynya. *MONTHLY WEATHER REVIEW*, *108*(12), 2032–2044. https://doi.org/10.1175/1520-0493(1980)108<2032:MOOTWP>2.0.CO;2

Cheon, W. G., Cho, C. B., Gordon, A. L., Kim, Y. H., & Park, Y. G. (2018). The Role of Oscillating Southern Hemisphere Westerly Winds: Southern Ocean Coastal and Open-Ocean Polynyas. *Journal of Climate*, *31*(3), 1053–1073. https://doi.org/10.1175/JCLI-D-17-0237.1

Cheon, W. G., & Gordon, A. L. (2019). Open-ocean polynyas and deep convection in the Southern Ocean. *Scientific Reports 2019 9:1*, *9*(1), 1–9. https://doi.org/10.1038/s41598-019-43466-2

Chu, P. C. ., & Gascard, J. C. . (1991). Deep convection and deep water formation in the oceans : proceedings of the International Monterey Colloquium on Deep Convection and Deep Water Formation in the Oceans. 382.

Comiso, J. C. (1986). Characteristics of Arctic winter sea ice from satellite multispectral microwave observations. *Journal of Geophysical Research*, *91*(C1), 975–994. https://doi.org/10.1029/JC091IC01P00975;PAGE:STRING:ARTICLE/CHAPTER

Comiso, J. C., & Gordon, A. L. (1987). Recurring polynyas over the Cosmonaut Sea and the Maud Rise. *Journal of Geophysical Research: Oceans*, *92*(C3), 2819–2833. https://doi.org/10.1029/JC092IC03P02819

Comiso, J. C., & Gordon, A. L. (1996). Cosmonaut polynya in the Southern Ocean: Structure and variability. *Journal of Geophysical Research: Oceans*, *101*(C8), 18297–18313. https://doi.org/10.1029/96JC01500

De Lavergne, C., Palter, J. B., Galbraith, E. D., Bernardello, R., & Marinov, I. (2014). Cessation of deep convection in the open Southern Ocean under anthropogenic climate change. *Nature Climate Change 2014 4:4*, *4*(4), 278–282. https://doi.org/10.1038/nclimate2132

Dong, S., Sprintall, J., Gille, S. T., & Talley, L. (2008). Southern Ocean mixed-layer depth from Argo float profiles. *Journal of Geophysical Research: Oceans*, *113*(C6). https://doi.org/10.1029/2006JC004051

Dorschel, B., Hehemann, L., Viquerat, S., Warnke, F., Dreutter, S., Tenberge, Y. S., Accettella, D., An, L., Barrios, F., Bazhenova, E., Black, J., Bohoyo, F., Davey, C., De Santis, L., Dotti, C. E., Fremand, A. C., Fretwell, P. T., Gales, J. A., Gao, J., … Arndt, J. E. (2022). The International Bathymetric Chart of the Southern Ocean Version 2. *Scientific Data 2022 9:1*, *9*(1), 1–13. [Dataset] https://doi.org/10.1038/s41597-022-01366-7

Dotto, T. S., Naveira Garabato, A., Bacon, S., Tsamados, M., Holland, P. R., Hooley, J., Frajka-Williams, E., Ridout, A., & Meredith, M. P. (2018). Variability of the Ross Gyre, Southern Ocean: Drivers and Responses Revealed by Satellite Altimetry. *Geophysical Research Letters*, *45*(12), 6195–6204. https://doi.org/10.1029/2018GL078607

Dragomir, O. C. (2024). *Dynamics of the subpolar Southern Ocean response to climate change* [University of Southampton]. https://eprints.soton.ac.uk/492038/

Dutta, S. (2025). *deep080/Cosmonaut-Sea-Paper: Initial Release* [Software]. Zenodo. https://doi.org/10.5281/zenodo.17497007

Ferreira, D., Marshall, J., Bitz, C. M., Solomon, S., & Plumb, A. (2015). Antarctic Ocean and Sea Ice Response to Ozone Depletion: A Two-Time-Scale Problem. *Journal of Climate*, *28*(3), 1206–1226. https://doi.org/10.1175/JCLI-D-14-00313.1

Fogt, R. L., & Marshall, G. J. (2020). The Southern Annular Mode: Variability, trends, and climate impacts across the Southern Hemisphere. *Wiley Interdisciplinary Reviews: Climate Change*, *11*(4), e652. https://doi.org/10.1002/WCC.652

Francis, D., Eayrs, C., Cuesta, J., & Holland, D. (2019). Polar Cyclones at the Origin of the Reoccurrence of the Maud Rise Polynya in Austral Winter 2017. *Journal of Geophysical Research: Atmospheres*, *124*(10), 5251–5267. https://doi.org/10.1029/2019JD030618

Geddes, J. A., & Moore, G. W. K. (2007). A climatology of sea ice embayments in the Cosmonaut Sea, Antarctica. *Geophysical Research Letters*, *34*(2), 2505. https://doi.org/10.1029/2006GL027910

Goosse, H., & Fichefet, T. (2001). Open-ocean convection and polynya formation in a large-scale ice-ocean model. *Tellus A*, *53*(1), 94–111. https://doi.org/10.1034/J.1600-0870.2001.01061.X

Gordon, A. L., & Huber, B. A. (1995). Warm Weddell Deep Water west of Maud Rise. *Journal of Geophysical Research: Oceans*, *100*(C7), 13747–13753. https://doi.org/10.1029/95JC01361

Harris, P. T., & Whiteway, T. (2011). Global distribution of large submarine canyons: Geomorphic differences between active and passive continental margins. *Marine Geology*, *285*(1–4), 69–86. https://doi.org/10.1016/J.MARGEO.2011.05.008

Haumann, F. A., Gruber, N., & Münnich, M. (2020). Sea-Ice Induced Southern Ocean Subsurface Warming and Surface Cooling in a Warming Climate. *AGU Advances*, *1*(2), e2019AV000132. https://doi.org/10.1029/2019AV000132

Holland, D. M. (2001). Explaining the Weddell Polynya - A large ocean eddy shed at Maud Rise. *Science*, *292*(5522), 1697–1700. https://doi.org/10.1126/SCIENCE.1059322/SUPPL_FILE/SUPPLEMENT.HTML

Hoppema, M., & Anderson, L. G. (2007). Chapter 6 Biogeochemistry of Polynyas and Their Role in Sequestration of Anthropogenic Constituents. *Elsevier Oceanography Series*, *74*, 193–221. https://doi.org/10.1016/S0422-9894(06)74006-5

Jena, B., Bajish, C. C., Turner, J., Ravichandran, M., Anilkumar, N., & Kshitija, S. (2022). Record low sea ice extent in the Weddell Sea, Antarctica in April/May 2019 driven by intense and explosive polar cyclones. *Npj Climate and Atmospheric Science 2022 5:1*, *5*(1), 1–15. https://doi.org/10.1038/s41612-022-00243-9

Jena, B., Ravichandran, M., & Turner, J. (2019). Recent Reoccurrence of Large Open-Ocean Polynya on the Maud Rise Seamount. *Geophysical Research Letters*, *46*(8), 4320–4329. https://doi.org/10.1029/2018GL081482

Lewis, E. L. (1980). The Practical Salinity Scale 1978 and Its Antecedents. *IEEE Journal of Oceanic Engineering*, *5*(1), 3–8. https://doi.org/10.1109/JOE.1980.1145448

Li, Y., Ji, R., Jenouvrier, S., Jin, M., & Stroeve, J. (2016). Synchronicity between ice retreat and phytoplankton bloom in circum-Antarctic polynyas. *Geophysical Research Letters*, *43*(5), 2086–2093. https://doi.org/10.1002/2016GL067937

Lin, Y., Nakayama, Y., Liang, K., Huang, Y., Chen, D., & Yang, Q. (2024). A dataset of the daily edge of each polynya in the Antarctic. *Scientific Data 2024 11:1*, *11*(1), 1–14. https://doi.org/10.1038/s41597-024-03848-2

Markus, T. (2000). An enhancement of the NASA team sea ice algorithm. *IEEE Transactions on Geoscience and Remote Sensing*, *38*(3), 1387–1398. https://doi.org/10.1109/36.843033

Maykut, G. A., & McPhee, M. G. (1995). Solar heating of the Arctic mixed layer. *Journal of Geophysical Research: Oceans*, *100*(C12), 24691–24703. https://doi.org/10.1029/95JC02554

Maykut, G. A., & Perovich, D. K. (1987). The role of shortwave radiation in the summer decay of a sea ice cover. *Journal of Geophysical Research: Oceans*, *92*(C7), 7032–7044. https://doi.org/10.1029/JC092IC07P07032

Mo, R. (2024). EDARA: An ERA5-based Dataset for Atmospheric River Analysis. *Scientific Data*, *11*(1), 1–14. https://doi.org/10.1038/S41597-024-03679-1;SUBJMETA=106,172,35,4081,704;KWRD=ATMOSPHERIC+SCIENCE,ENVIRONMENTAL+IMPACT

Morales Maqueda, M. A., Willmott, A. J., & Biggs, N. R. T. (2004). Polynya Dynamics: a Review of Observations and Modeling. *Reviews of Geophysics*, *42*(1). https://doi.org/10.1029/2002RG000116

Narayanan, A., Roquet, F., Gille, S. T., Gülk, B., Mazloff, M. R., Silvano, A., & Garabato, A. C. N. (2024). Ekman-driven salt transport as a key mechanism for open-ocean polynya formation at Maud Rise. *Science Advances*, *10*(18). https://doi.org/10.1126/SCIADV.ADJ0777/SUPPL_FILE/SCIADV.ADJ0777_SM.PDF

Nihashi, S., & Ohshima, K. I. (2015). Circumpolar Mapping of Antarctic Coastal Polynyas and Landfast Sea Ice: Relationship and Variability. *Journal of Climate*, *28*(9), 3650–3670. https://doi.org/10.1175/JCLI-D-14-00369.1

Ohshima, K. I., Nihashi, S., & Iwamoto, K. (2016). Global view of sea-ice production in polynyas and its linkage to dense/bottom water formation. *Geoscience Letters*, *3*(1), 1–14. https://doi.org/10.1186/S40562-016-0045-4/FIGURES/5

Orsi, A. H., Whitworth, T., & Nowlin, W. D. (1995a). On the meridional extent and fronts of the Antarctic Circumpolar Current. *Deep Sea Res. Part I*, *42*(5), 641–673. https://doi.org/10.1016/0967-0637(95)00021-w

Orsi, A. H., Whitworth, T., & Nowlin, W. D. (1995b). On the meridional extent and fronts of the Antarctic Circumpolar Current. *Deep Sea Research Part I: Oceanographic Research Papers*, *42*(5), 641–673. https://doi.org/10.1016/0967-0637(95)00021-W

Park, J., Kim, H. C., Jo, Y. H., Kidwell, A., & Hwang, J. (2018). Multi-temporal variation of the Ross Sea Polynya in response to climate forcings. *Polar Research*, *37*(1). https://doi.org/10.1080/17518369.2018.1444891;SUBPAGE:STRING:FULL

Perovich, D. K., & Richter-Menge, J. A. (2000). Ice growth and solar heating in springtime leads. *Journal of Geophysical Research: Oceans*, *105*(C3), 6541–6548. https://doi.org/10.1029/1999JC900321

Prasad, T. G., McClean, J. L., Hunke, E. C., Semtner, A. J., & Ivanova, D. (2005). A numerical study of the western Cosmonaut polynya in a coupled ocean–sea ice model. *Journal of Geophysical Research: Oceans*, *110*(C10), 1–21. https://doi.org/10.1029/2004JC002858

Roquet, F., Ferreira, D., Caneill, R., Schlesinger, D., & Madec, G. (2022). Unique thermal expansion properties of water key to the formation of sea ice on Earth. *Science Advances*, *8*(46), 793. https://doi.org/10.1126/SCIADV.ABQ0793/SUPPL_FILE/SCIADV.ABQ0793_SM.PDF

Sallée, J. B., Speer, K., & Morrow, R. (2008). Response of the Antarctic Circumpolar Current to Atmospheric Variability. *Journal of Climate*, *21*(12), 3020–3039. https://doi.org/10.1175/2007JCLI1702.1

Shadwick, E. H., Tilbrook, B., & Currie, K. I. (2017). Late-summer biogeochemistry in the Mertz Polynya: East Antarctica. *Journal of Geophysical Research: Oceans*, *122*(9), 7380–7394. https://doi.org/10.1002/2017JC013015

Smith, S. D., Muench, R. D., & Pease, C. H. (1990). Polynyas and leads: An overview of physical processes and environment. *Journal of Geophysical Research: Oceans*, *95*(C6), 9461–9479. https://doi.org/10.1029/JC095IC06P09461

Spreen, G., Kaleschke, L., & Heygster, G. (2008a). Sea ice remote sensing using AMSR-E 89-GHz channels. *Journal of Geophysical Research: Oceans*, *113*(2), 2–03. https://doi.org/10.1029/2005JC003384;SUBPAGE:STRING:FULL

Spreen, G., Kaleschke, L., & Heygster, G. (2008b). Sea ice remote sensing using AMSR-E 89-GHz channels. *Journal of Geophysical Research: Oceans*, *113*(C2). [Dataset] https://doi.org/10.1029/2005JC003384

Stammer, D. (1998). On Eddy Characteristics, Eddy Transports, and Mean Flow Properties. *Journal of Physical Oceanography*, *28*(4), 727–739. https://doi.org/10.1175/1520-0485(1998)028

Tamura, T., Ohshima, K. I., & Nihashi, S. (2008). Mapping of sea ice production for Antarctic coastal polynyas. *Geophysical Research Letters*, *35*(7), 7606. https://doi.org/10.1029/2007GL032903

Tamura, T., Ohshima, K. I., Nihashi, S., & Hasumi, H. (2011). Estimation of Surface Heat/Salt Fluxes Associated with Sea Ice Growth/Melt in the Southern Ocean. *SOLA*, *7*(1), 17–20. https://doi.org/10.2151/SOLA.2011-005

Thompson, A. F., Heywood, K. J., Schmidtko, S., & Stewart, A. L. (2014). Eddy transport as a key component of the Antarctic overturning circulation. *Nature Geoscience 2014 7:12*, *7*(12), 879–884. https://doi.org/10.1038/ngeo2289

Uotila, P., Vihma, T., & Tsukernik, M. (2013). Close interactions between the Antarctic cyclone budget and large-scale atmospheric circulation. *Geophysical Research Letters*, *40*(12), 3237–3241. https://doi.org/10.1002/GRL.50560

Van Der Walt, S., Schönberger, J. L., Nunez-Iglesias, J., Boulogne, F., Warner, J. D., Yager, N., Gouillart, E., & Yu, T. (2014). Scikit-image: Image processing in python. *PeerJ*, *2014*(1), e453. https://doi.org/10.7717/PEERJ.453/FIG-5

Wei, Z., Zhang, Z., Vihma, T., Wang, X., & Chen, Y. (2021). An overview of antarctic polynyas: Sea ice production, forcing mechanisms, temporal variability and water mass formation. In *Advances in Polar Science* (Vol. 32, Issue 4, pp. 292–308). Editorial Office of Advances in Polar Science. https://doi.org/10.13679/j.advps.2021.0026

Wei, Z., Zhang, Z., Wang, X., Chen, Y., & Zhou, M. (2022). The thermodynamic and dynamic control of the sensible heat polynya in the western Cosmonaut Sea. *Deep Sea Research Part II: Topical Studies in Oceanography*, *195*, 105000. https://doi.org/10.1016/j.dsr2.2021.105000

Weijer, W., Veneziani, M., Stössel, A., Hecht, M. W., Jeffery, N., Jonko, A., Hodos, T., & Wang, H. (2017). Local Atmospheric Response to an Open-Ocean Polynya in a High-Resolution Climate Model. *Journal of Climate*, *30*(5), 1629–1641. https://doi.org/10.1175/JCLI-D-16-0120.1

Wong, A. P. S., Wijffels, S. E., Riser, S. C., Pouliquen, S., Hosoda, S., Roemmich, D., Gilson, J., Johnson, G. C., Martini, K., Murphy, D. J., Scanderbeg, M., Bhaskar, T. V. S. U., Buck, J. J. H., Merceur, F., Carval, T., Maze, G., Cabanes, C., André, X., Poffa, N., … Park, H. M. (2020). Argo Data 1999–2019: Two Million Temperature-Salinity Profiles and Subsurface Velocity Observations From a Global Array of Profiling Floats. *Frontiers in Marine Science*, *7*, 568494. [Dataset] https://doi.org/10.3389/FMARS.2020.00700/BIBTEX

Yang, S., Zhou, M., & Cheng, X. (2024). Seasonal and Interannual Variability Between Upper Ocean Processes and the Slope Current in the Region Around the Cosmonauts Sea Off East Antarctica. *Journal of Geophysical Research: Oceans*, *129*(2), e2023JC019636. https://doi.org/10.1029/2023JC019636

Zanowski, H., Hallberg, R., & Sarmiento, J. L. (2015). Abyssal Ocean Warming and Salinification after Weddell Polynyas in the GFDL CM2G Coupled Climate Model. *Journal of Physical Oceanography*, *45*(11), 2755–2772. https://doi.org/10.1175/JPO-D-15-0109.1

Zhou, L., Heuzé, C., & Mohrmann, M. (2023). Sea Ice Production in the 2016 and 2017 Maud Rise Polynyas. *Journal of Geophysical Research: Oceans*, *128*(2), e2022JC019148. https://doi.org/10.1029/2022JC019148